LIMNOLOGY
and
OCEANOGRAPHY

ASLO

Limnol. Oceanogr. 00, 2017, 00–00

doi: 10.1002/lno.10649

Water column and sediment stable carbon isotope biogeochemistry of permanently redox-stratified Fayetteville Green Lake, New York, U.S.A.

Jeff R. Havig [1,a]* Trinity L. Hamilton [2] Michael McCormick,[3] Brianna McClure,[1] Todd Sowers,[1] Bruce Wegter,[3] Lee R. Kump[1]

[1]Department of Geosciences and the Penn State Astrobiology Research Center, The Pennsylvania State University, University Park, Pennsylvania
[2]Department of Plant and Microbial Biology, University of Minnesota, St. Paul, Minnesota
[3]Department of Biology, Hamilton College, Clinton, New York

Abstract

Carbon cycling in natural ecosystems is a biologically mediated process with global consequences. Recent work has revealed the important role that lakes play in the global carbon cycle, suggesting organic carbon burial in small lakes and reservoirs matching and even surpassing that of the world's oceans. While much is known regarding biogeochemical cycling of carbon in the water column and underlying sediments of freshwater and marine systems, less is known about permanently redox-stratified water bodies. The modern ocean is fully oxygenated, however, the ocean is thought to have been redox-stratified throughout much of Earth's history, and seasonal redox-stratification is an increasing problem in many freshwater systems due to eutrophication driven by human land usage and warming resulting from global climate change. To better understand carbon signals preserved in the rock record from times of ocean redox-stratification as well as the effects of increasing redox-stratification on carbon cycling in modern freshwater systems, we have characterized the concentration and stable isotopic signal of inorganic and organic carbon in permanently redox-stratified Fayetteville Green Lake (FGL), New York. The results of these analyses indicate that: (1) groundwater is the primary source of dissolved inorganic carbon (DIC) at FGL; (2) organic carbon is extensively cycled within the water column and upper sediments resulting in an increasingly isotopically depleted DIC pool; (3) cyanobacteria-driven carbonate precipitation in the oxic zone is the primary source of carbonate in the sediments; (4) methane concentrations increase below the chemocline with extremely negative $\delta^{13}C$ values (−99.1‰ to −102.3‰).

Stable carbon isotopic signals preserved in carbonate rocks and organic carbon reflect environmental conditions at the time of deposition, and record results of carbon cycling driven by an ever changing Earth surface and evolving biosphere. Recent work on carbon sequestration in lake and reservoirs has focused on mass balance and total organic carbon (e.g., Downing et al. 2008; Tranvik et al. 2009; Kastowski et al. 2011; Dong et al. 2012; Heathcote and Downing 2012; Anderson et al. 2013; Anderson et al. 2014), with results indicating lakes, reservoirs, and ponds may sequester 1.4–3.7 times as much organic carbon as the world's oceans (Downing et al. 2008). Previous work has shown the value of quantifying carbon isotope values of inorganic and organic carbon pools in lakes for tracking the flow of carbon through these systems (e.g., Fry and Sherr 1989; Schindler et al. 1997; Kritzberg et al. 2004). Global climate change is expected to increase the occurrence of stratification in lake and reservoirs which results in anoxic conditions in the bottom layer of the water column (Paerl and Huisman 2009). This underscores the need for quantifying inorganic and organic carbon pools in permanently redox stratified systems. Furthermore, redox-stratified systems were more common in Earth's past thus modern redox-stratified systems serves as analog for interpreting carbon isotope signals preserved in the rock record.

In the context of modern, natural environments, Fayetteville Green Lake (FGL), New York is a peculiar, redox-stratified, freshwater system supporting abundant microbial

*Correspondence: jeffhavig@gmail.com

[a]Present address: Department of Earth Sciences, University of Minnesota, Minneapolis, Minnesota

Additional Supporting Information may be found in the online version of this article.

life (Fig. 1). FGL is located in the gypsum-bearing Vernon Shale charged with groundwater that is replete in sulfate (Deevey et al. 1963). Continuous input of sulfate and organic carbon into FGL supports sulfate reduction in the monimolimnion and sediments resulting in a monimolimnion that is perennially euxinic (sulfide-rich), and an oxic/euxinic boundary that hosts a phototrophic microbial plate (dense floating layer of microbial biomass). In FGL, this boundary (at $\sim$ 20.5 m) is inhabited by cyanobacteria, purple sulfur bacteria (PSB), and green sulfur bacteria (GSB) (Hunter 2012). In addition, dramatic changes in Mn, Fe, and Mo concentrations occur across the oxic/euxinic transition. These conditions are similar to those thought to have been prevalent during the Proterozoic (Meyer and Kump 2008; Havig et al. 2015) but are not widespread today.

FGL is supersaturated in the oxic zone with respect to calcite and dissolved inorganic carbon (DIC) concentration increases while $\delta^{13}C$ values decrease with depth in the water column (Eggleton 1956; Deevey et al. 1963; Takahashi et al. 1968; Brunskill and Ludlam 1969; Torgersen et al. 1981; Havig et al. 2015). The dissolved organic carbon (DOC) concentration is relatively unchanged throughout the water column (Havig et al. 2015) while the particulate organic carbon (POC), or seston, has more negative $\delta^{13}C$ values at and below the chemocline relative to the oxic zone (Fry 1986; Fulton 2010). The concentration of organic carbon in sediment is classified as a sapropel ($>$ 2% organic carbon) with $\delta^{13}C$ values between $-26‰$ and $-34‰$ (Fry 1986; Hilfinger et al. 2001; Fulton 2010). Carbonates are the dominant mineral in the sediments with $\delta^{13}C$ values between $-3.4‰$ and $-5.6‰$ (Takahashi et al. 1968; Hilfinger et al. 2001; Fulton 2010).

Carbon in natural systems exists in many different forms including DIC, DOC, and POC, with the difference between particulate and dissolved operationally based on the pore size of the filters used (0.22 μm for this study). DIC is typically the primary source of carbon for primary productivity and carbonate precipitation in natural waters. The concentration and isotopic value of DIC is influenced by biological activity (e.g., C-fixation, microbial respiration) and inorganic processes (e.g., mixing, carbonate precipitation, weathering, air/water gas exchange). DOC encompasses a variety of organic compounds ranging from those that are very labile and experience rapid turnover, generally being consumed as quickly as they are produced (e.g., sugars, amino acids, short-chained fatty acids), to refractory organic carbon that is recalcitrant and can experience turnover timescales of millennia (Hansell 2013). POC is assumed to be predominantly made up of microbial biomass, though it also contains dead and decaying planktonic organic material, allochthonous plant material, and fecal material from zooplankton and macrofauna. The cycling of carbon between DIC, DOC, and POC pools is predominantly biologically mediated, and the accumulation of POC in sediments is one of the primary drivers maintaining the oxidized state of the Earth's surface. The concentration and carbon isotope signal of this material integrates all of the processes that influence the movement of carbon through the water column and deposition as sediments (as well as movement of carbon from sediments back into the water column) that can be incorporated into the rock record. Using these data, we can better constrain the redox history of the ancient oceans and predict the effects increasing phytoplankton blooms and resulting anoxia have on carbon cycling and burial in terrestrial lakes and reservoirs.

In this study, we expand on this body of knowledge to build a more complete conceptual model of the carbon cycle in the water column and sediments at FGL. We report the carbon isotopic values of DIC, DOC, POC, and methane in the FGL water column; DIC and DOC of sediment pore water; organic and inorganic carbon in sediments; and DIC and DOC for inputs into the lake (e.g., groundwater and surface inflow). From this data set, we show the effects of carbon cycling on the carbon isotope systematics in a permanently redox stratified lake and present a conceptual model for the movement of carbon in FGL. Finally, we relate our findings at FGL to increasing anoxia in lakes and reservoirs due to global climate change and perspectives on periods of redox stratification in the ancient ocean.

Methods

Samples were collected during sampling trips on 10–11 November 2012, 09 June 2013, 16–19 July 2013, 17–18 July 2014, and 13–17 July 2015. High-density water column sampling and sample processing was conducted as described in McCormick et al. (2014), and subset samples were collected via peristaltic pump (attached to a sonde to verify depth) or 3.8 L Van Dorn bottle. Geochemical and physical analysis methods were followed as described previously, with results from 2012 and 2013 samples reported in Havig et al. (2015), and results are summarized in Figs. 2–7. Temperature, pH, conductivity, optical dissolved oxygen, oxidation-reduction potential (ORP), turbidity, and depth were determined for the full water column using a calibrated YSI 6600 multiparameter sonde probe (YSI, Yellow Springs, Ohio). ORP values reported in mV relative to the Ag/AgCl electrode. Water samples were filtered through 0.22 μm polyethersulfone syringe filters (VWR International). Anion (SO_4^{2-}, Cl^-) concentrations for samples collected in 2015 were determined via ion chromatography and cation (Ca^{2+}, Mg^{2+}, Na^+) and trace element (P) concentrations via inductively coupled plasma optical emission spectrometry by the Star Lab (Ohio State University, Columbus, Ohio). Additional water samples were collected from the input stream fed by outflow from Round Lake, the outlet draining FGL, and a sulfidic groundwater-fed spring located near Chittenango, New York. Temperature, pH, and conductivity for these samples were determined using a WTW 3110 pH meter and a YSI Pro30 conductivity meter. Sediment cores were collected at a depth

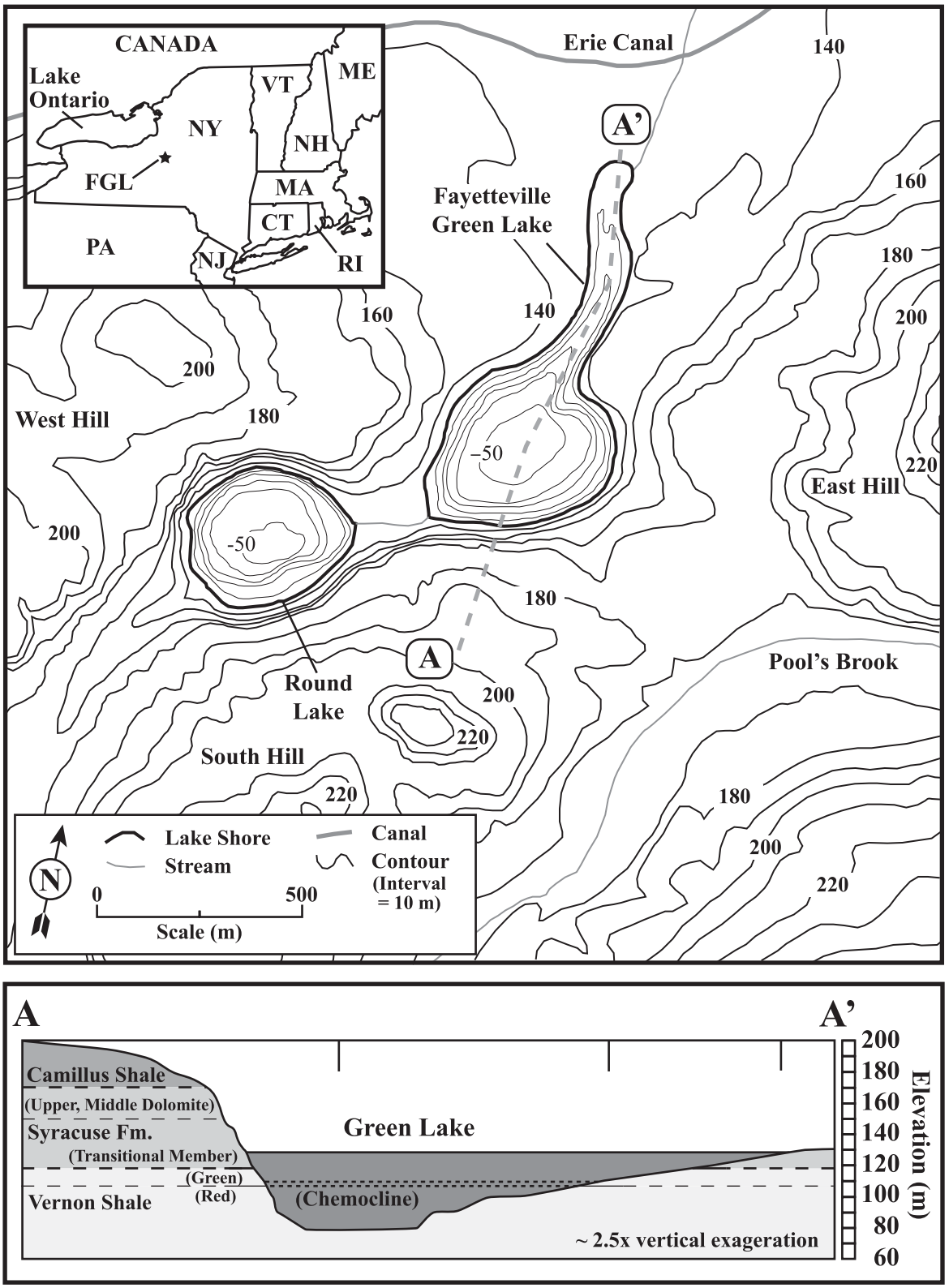

Fig. 1. Map and cross section of FGL, New York, modified from Muller (1967), Takahashi et al. (1968), Jelacic (1970), Hilfinger et al. (2001), and Havig et al. (2015). Letters and dashed gray lines denote cross section. Vertical lines in cross section denote deviation from a straight line between A and A'.

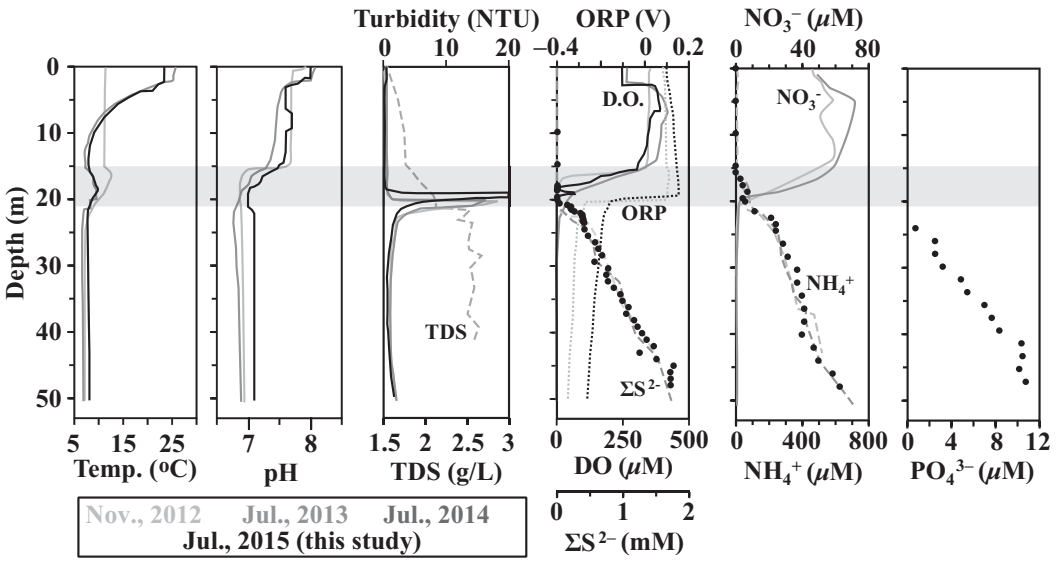

Fig. 2. Water geochemistry and physical parameters plotted against depth for FGL, modified from Havig et al. (2015). Water temperature (Temp.), pH, turbidity, ORP, and optical dissolved oxygen (DO) measured via SONDE. Total dissolved solids reported by Havig et al. (2015). Gray lines represent values from 10 November 2012, black lines from 16 July 2013. Turbidity in nephelometric turbidity units (NTU), and ORP in volts. Gray shaded region represents the chemocline. Data points denote new discrete sample analyses.

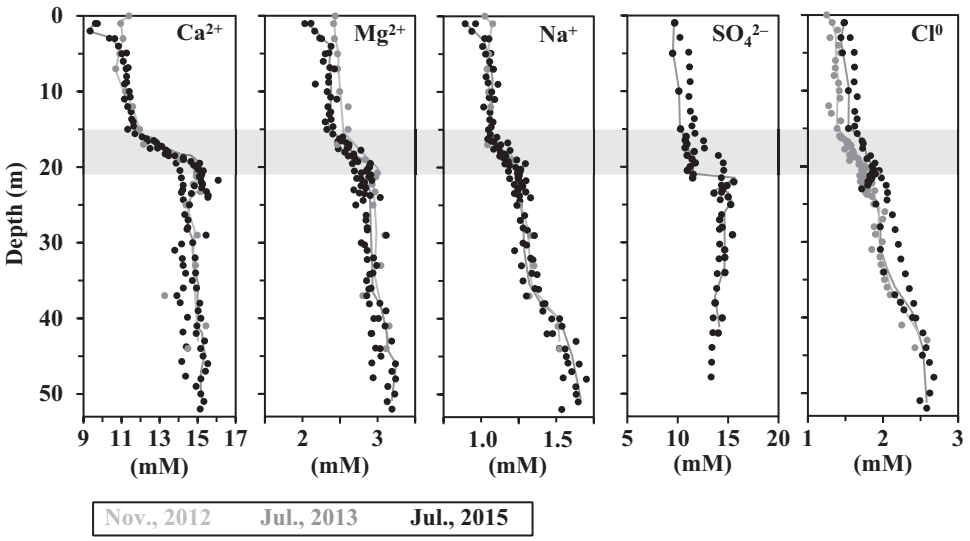

Fig. 3. Major cation and anion concentrations plotted against depth from surface for FGL, New York, modified from Havig et al. (2015). Gray lines represent values from November 2012, and July 2013, and black filled circles from July 2015. Gray shaded region represents the chemocline.

of 53 m using a gravity corer fitted with clear 50 cm long, 5 cm diameter polycarbonate liners. Sediment cores were immediately sealed with caps that were fixed in place with electrician's tape, kept upright, and either placed on dry ice until they were returned to the lab where they were stored at −20°C until processed or kept on ice and processed upon return to the lab for pore-water samples. Sediment subsamples were collected by extrusion and sectioning into a N_2-filled and positive pressure glove box. Pore water was recovered by centrifugation of sediments in gas tight Oak Ridge tubes (5000 rpm at 4°C for 10 min) with a N_2 headspace, and supernatant water was drawn into a syringe and filtered through a 0.22 μm polyethersulfone syringe filter and distributed into appropriate sample containers as described previously (McCormick et al. 2014; Havig et al. 2015). A core collected in November of 2012 was divided into 3 cm sections for analysis of pore-water CH_4 concentration, and a core collected in July of 2015 was divided into 2–4 cm sections for pore-water analyses. Cores in November 2012 and July of 2013 were used for incubation and DNA extraction at Penn State University. For detailed descriptions of

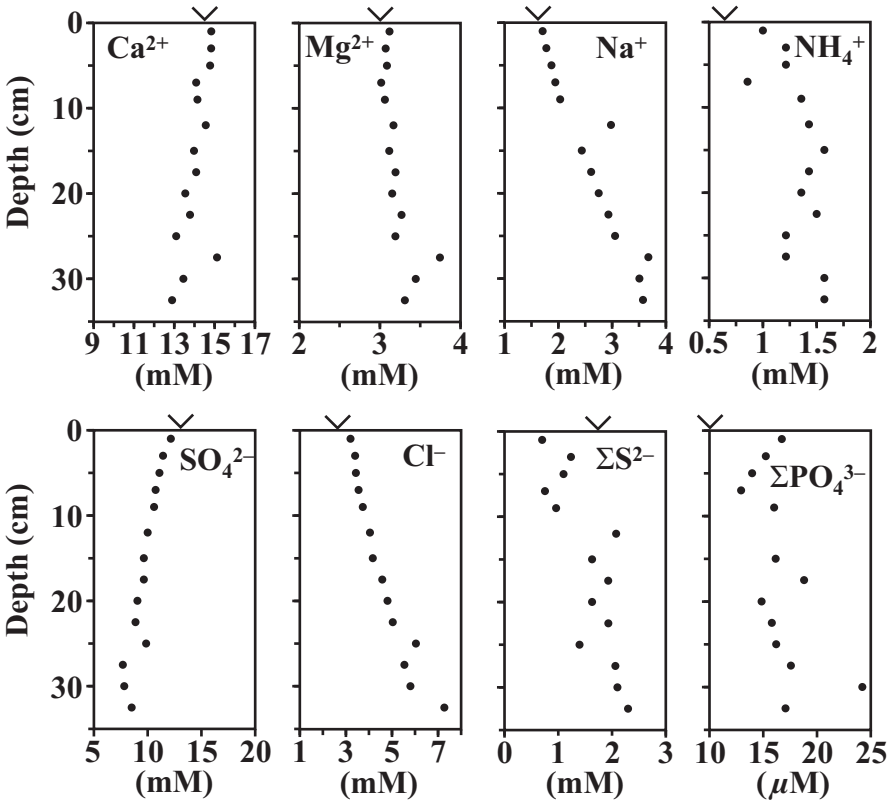

Fig. 4. Geochemistry measured in samples collected in July 2015 from sediment pore water of FGL, New York, plotted against depth from sediment surface/water column interface. Black filled circles represent samples from July 2015. Carrots at the top of plots indicate values for overlying water when known.

physical and geochemical methods used, please see the Supporting Information Material.

All stable carbon isotope results are given in delta formation expressed as per mil (‰):

$$\delta^{13}C = \left[\left((R_a)_{sample}/(R_a)_{standard}\right) - 1\right] \times 10^3 \quad (1)$$

where R_a is the $^{13}C/^{12}C$ ratio of the sample or standard, and are reported vs. the Vienna Pee Dee Belemnite (VPDB) standard.

DNA extractions and polymerase chain reaction (PCR) amplifications were carried out on filters containing water column biomass and on bulk sediments collected from the top 50 cm to test for the presence of methanogens, with the details of collection and methods used reported in the Supporting Information Material. Methane production microcosms were inoculated with biomass collected via filtration from the water column or bulk sediments collected from the top 50 cm, with the details of setup and analysis reported in the Supporting Information Material.

Results

Water column geochemistry

Water column physical and geochemical parameters measured in 2015 (temperature, pH, turbidity, ORP, dissolved oxygen, ammonium, calcium, magnesium, sodium, sulfate, and chloride) were similar to values that have been reported previously (Havig et al. 2015), and consistent with previous work indicating FGL is meromictic (Eggleton 1931). The water column is stratified with an oxic mixolimnion and a euxinic monimolimnion. A mixing zone characterized by multiple chemical gradients is observed between 15 m and 21 m (chemocline) and a redox transition zone (redoxcline) occurs near 20.5 m.

Water column carbon

Dissolved carbon concentrations and stable carbon isotopic values for DIC, DOC, and CH_4 in the FGL water column had similar patterns in samples collected in November 2012, July 2013, July 2014, and July 2015 (Fig. 5). DIC concentration increased with depth, from concentrations near or below 4 mM in the mixolimnion to a high of 9 mM in the deepest samples from the monimolimnion, while DIC $\delta^{13}C$ values became increasingly negative with increasing depth, with values at or above −9‰ in the mixolimnion to a low of −21.3‰ in the monimolimnion. DOC concentration was slightly elevated in the mixolimnion compared to the rest of the water column. Carbon isotope values for DOC, while exhibiting some scatter, seemed to show a general trend of $\delta^{13}C$ values around −31‰ through the mixolimnion, slightly

lower (−32‰) in the chemocline, and slightly higher in the monimolimnion (ca. −30‰ in the upper monimolimnion, ca. −31‰ in the lower monimolimnion).

Seston carbon content of filter-concentrated biomass (> 0.22 μm) from the FGL water column had $\delta^{13}C$ values of −27.1‰ (± 1.6) at 0 m, −32.1‰ (± 2.8) at 10 m, −36.8‰ (± 0.9) at 18 m, −40.0‰ (± 0.1) at 20.5 m, −34.5‰ (± 2.3) at 24 m, and −37.0‰ (± 0.1) at 30 m (Supporting Information Material). Suspended carbonate collected via filtration from 0 m and 10 m depths had $\delta^{13}C$ values of −5.4‰ and −5.5‰, respectively.

Water column methane

Methane concentrations were consistently below 1 μM through the mixolimnion and the chemocline, with concentrations increasing coincident with a turbidity maximum associated with a thick purple sulfur bacterial plate occurring near the base of the chemocline (Fig. 2, Havig et al. 2015). In November of 2012, the CH_4 concentration increase occurred between 20.6 m and 20.9 m (Fig. 5), while in July of 2014, it was between 19.7 m and 19.9 m, and in July of 2015, it was between 19.8 m and 20.0 m. The shift up in the water column is consistent with a slight shallowing of the turbidity peak (bacterial plate). Methane concentration reached a maximum value of 23.5 μM (loss corrected, see note in "Methods" above) in the lower monimolimnion (Fig. 5). Methane $\delta^{13}C$ values in the monimolimnion were between −99.1‰ and −102.3‰, while a measurement at 10 m yielded a value of −66.2‰ consistent with mixing of monimolimnion methane and atmospheric methane ($\delta^{13}C$ value of −47.3‰).

Sediment pore-water geochemistry

Pore-water cation and anion concentrations were measured at regular intervals (2–4 cm) in the top 34 cm of sediments, and show several patterns (Fig. 4). Sodium and chloride concentration increases with sediment depth (from 1.7 mM Na and 3.2 mM Cl from 0 cm to 2 cm to 3.6 mM Na and 7.8 mM Cl from 31 cm to 34 cm). Ammonium concentrations increased with depth for the upper 15 cm, then decreased to 27 cm, and increased below 30 cm. Calcium (and to a lesser extent magnesium) concentration decreased with depth. Sulfate concentration decreased with depth while sulfide concentration increased. Phosphorous concentration varied between 12.9 μM and 24.2 μM, with an outlier of 45.6 μM at 10–14 cm. Single data points that vary dramatically from overall trends are assumed to be outliers.

Pore-water carbon

The sediment core collected from near the center of FGL (∼ 53 m) was 48 cm in total length, with dark brown sediments from 48 cm to 20 cm, and gray sediments from 20 cm to the surface. This color transition is consistent with European settlement and clear-cutting of the forest dated at approximately 1770 CE resulting in a shift in sedimentation

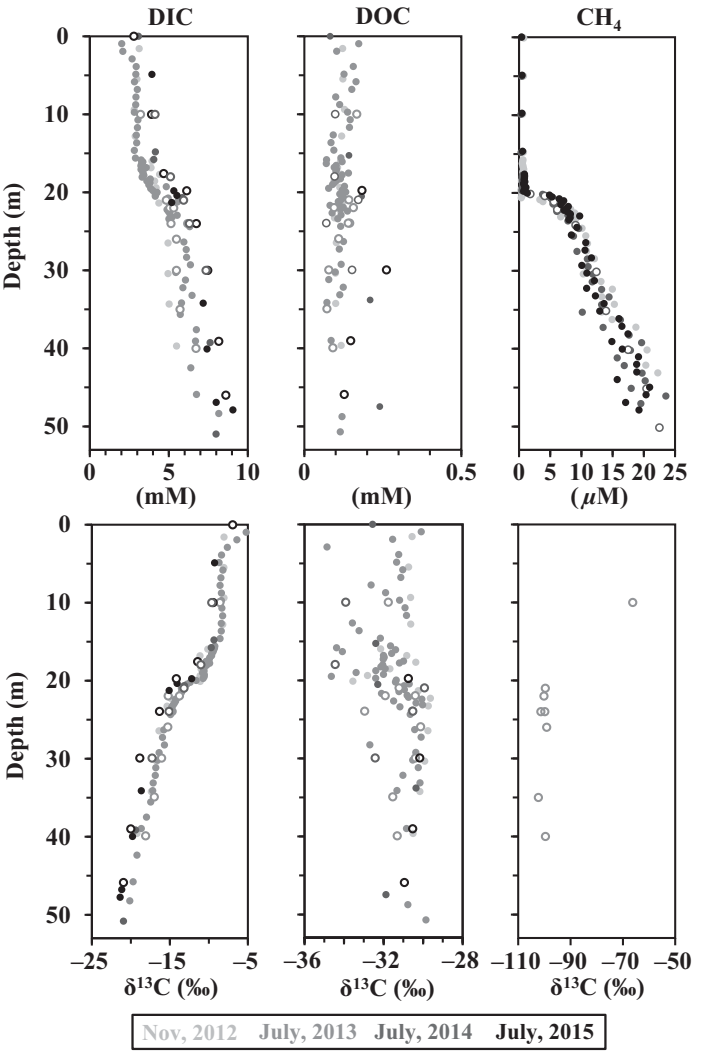

Fig. 5. DIC, DOC, and methane (CH_4) concentrations (top) and carbon stable isotope values (bottom) measured in samples collected from the water column of FGL, New York, plotted against depth from surface. DIC and DOC concentrations first reported in Havig et al. (2015). Filled symbols represent samples collected with the high-resolution sampler, open symbols for samples collected via peristaltic pump or Van Dorn bottle. All carbon isotope values are reported vs. VPDB standard, in units of per mil (‰).

rates from 0.1 mm/yr prior to 0.7 mm/yr following this time (Hilfinger et al. 2001). scanning electron microscope (SEM) imaging of sediments revealed larger carbonate crystals in the deeper sediments, and smaller carbonate crystals in sediments above ∼ 20 cm (Fig. 8). Sediment total carbonate concentration decreased from 82% total carbonate (wt. % $CaCO_3$, dry weight) at the surface to a minimum of 73% for the 15–20 cm depth range (Fig. 7). Values then increase to a maximum of 89% at the 25–30 cm depth range, and then decrease slightly with depth to 86% at the 40–48 cm depth range. Carbonate $\delta^{13}C$ values exhibit a low of −5.0‰ near the sediment/water interface to a high of −3.3‰ for the 25–

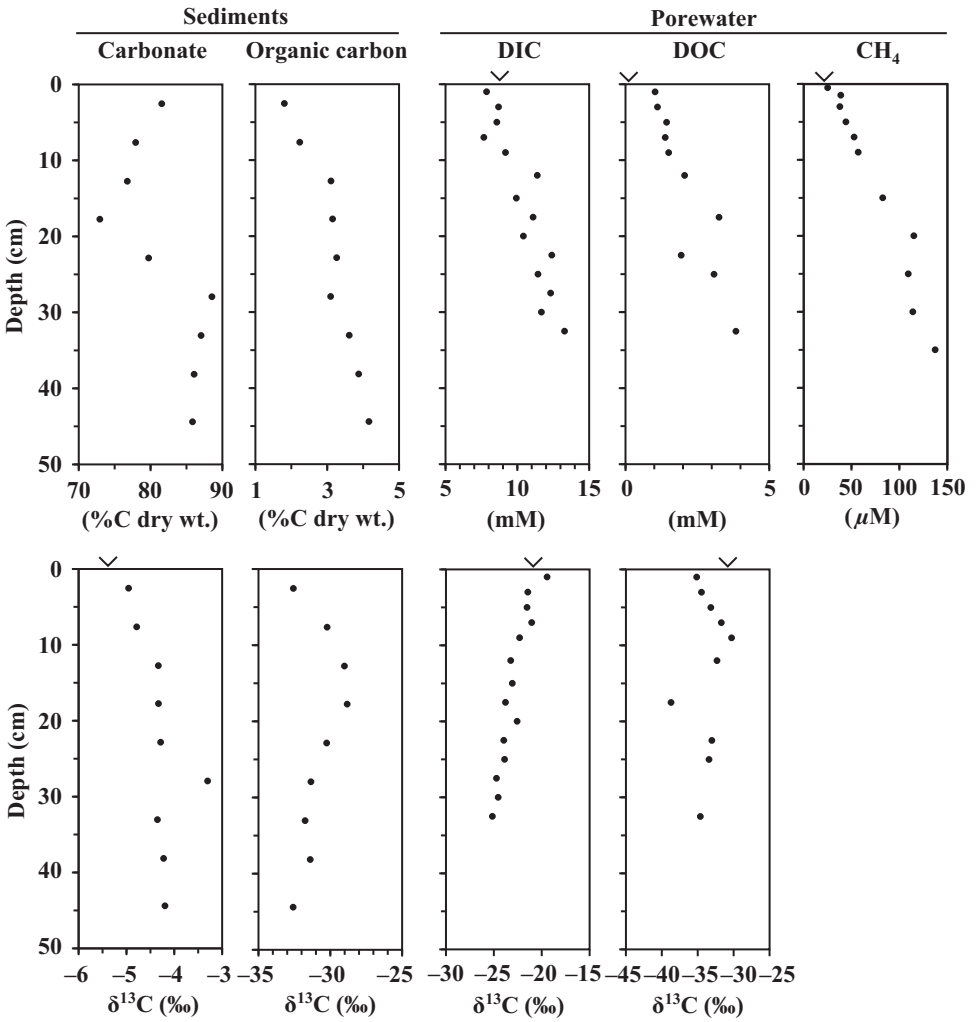

Fig. 6. Sediment (left) and pore-water (right) carbon and carbon isotope data from samples collected in 2015. Black filled circles represent samples from July 2015. Carrots at the top of plots indicate values for overlying water when known.

30 cm depth range, with an average value of −4.3‰ over the whole 48 cm depth range. Carbonate δ^{13}C values reported here agree with those reported for FGL sediments in previous work (Takahashi et al. 1968; Hilfinger et al. 2001). Sediment total organic carbon concentration increases with depth from a low of 1.8% organic carbon (wt. % organic C, dry weight) at the surface to a maximum of 4.2% for the 40–48 cm depth range. Organic carbon concentration was lower than that reported by Hilfinger et al. (2001), but is similar to that reported by Fulton (2010). Organic carbon δ^{13}C values increase from −32.6‰ at the surface to a high value of −28.8‰ for the 15–20 cm range, and then decrease to a low value of −32.6‰ for the 40–48 cm depth range, matching that of the surface, consistent with Fulton (2010).

Sediment core pore-water DIC concentration increases with depth, from values similar to the overlying monimolimnion water in the top 8 cm (~ 8 mM) to a maximum of 13.3 mM for the 31–34 cm depth interval (Fig. 6), concurrent with δ^{13}C values that are similar to the overlying water column DIC δ^{13}C values (pore-water value of −19.4‰, deep-water values of −20.1‰ to −21.4‰), and decreasing with depth to a minimum of −25.2‰ for the 31–34 cm interval. Sediment pore-water DOC concentration was the lowest over the 0–2 cm depth range (1.0 mM), and increased with depth to a highest value at the 31–34 cm depth interval (3.8 mM). Pore-water DOC δ^{13}C values ranged from −33.7‰ to −38.7‰. Sediment pore-water methane concentration increased from values similar to the overlying water column (25.2 μM) at the sediment-water interface to a maximum of 137.4 μM at the 32–38 cm depth range.

Other associated samples

Inflow from Round Lake (measured in July 2013)(Fig. 1) had a DIC concentration of 3.5 mM and a δ^{13}C value of −8.1‰ and a DOC concentration of 0.13 mM with a δ^{13}C value of −32.8‰. The outlet draining FGL (also measured in

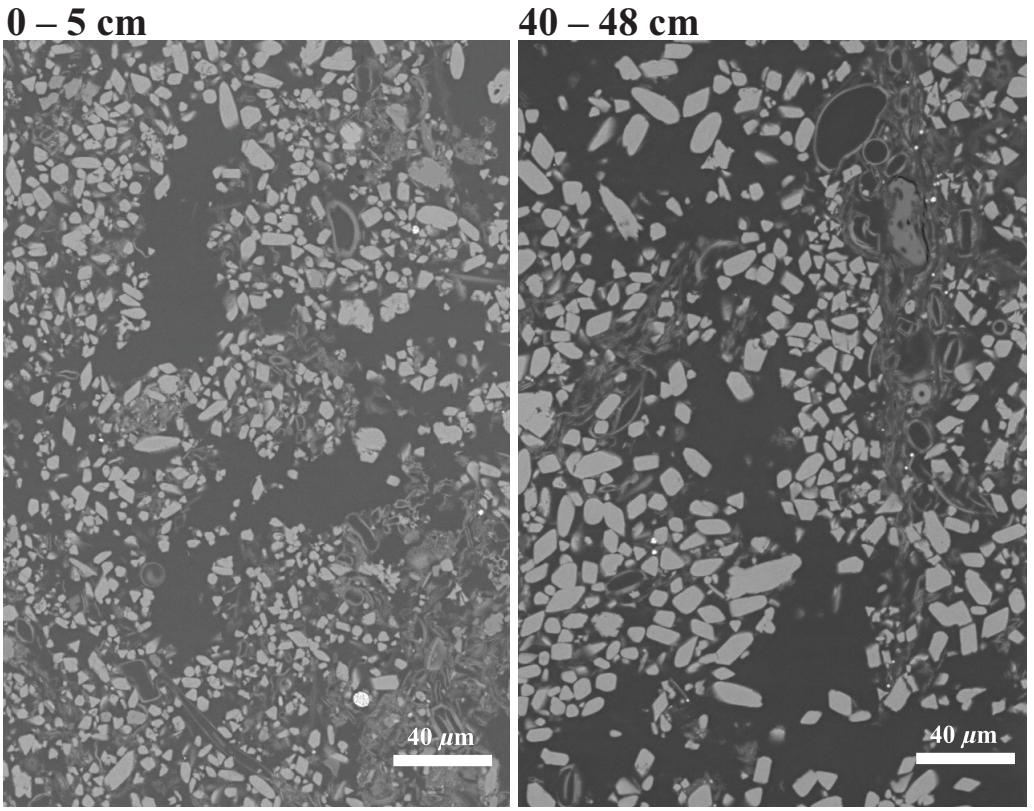

Fig. 7. Scanning electron microscope images of thin sections made from sediments collected from the top 5 cm (0–5 cm depth, left) and from the bottom 8 cm (40–48 cm depth, right) of a core collected from FGL in July 2015. Diatom frustules (SiO_2) show up as dark gray, carbonate crystals as light gray, and iron sulfide minerals as white. Field of view is identical for both images (note scale).

2013) had a DIC concentration of 2.9 mM with a $\delta^{13}C$ value of $-6.9‰$, and a DOC concentration of 0.12 mM with a $\delta^{13}C$ value of $-33.7‰$ (Table 1).

A groundwater fed sulfidic spring located $\sim$ 8 km from FGL (south of Chittenango, New York on highway 13) was sampled in 2015 as a presumed proxy for groundwater input into FGL. The spring pH (7.2), calcium (12.33 mM), sodium (1.18 mM), chloride (1.45 mM), and sulfate (15.84 mM) values were all similar to those found in the chemocline for FGL (Table 1). The spring had a DIC concentration of 4.9 mM and a $\delta^{13}C$ value of $-11.7‰$ and a DOC concentration of 0.07 mM with a $\delta^{13}C$ value of $-29.0‰$, also similar to the values found at the FGL chemocline.

Discussion

One-Dimensional box mixing models for DIC and CH_4

Comparing analytical results to the chloride concentration profile (a conservative tracer) indicates diffusion between a higher Cl concentration "deep source" from groundwater inputs in the monimolimnion and a lower Cl concentration "shallow water" source diluted by precipitation and surface runoff in the mixolimnion. Using this information, we built a simple 1-dimensional (1D) box mixing models for DIC and CH_4 to estimate potential sources and sinks in the water column.

Dissolved inorganic and organic carbon

DIC $\delta^{13}C$ values in the water column reflect three distinct layers (Fig. 5)—the chemocline DIC $\delta^{13}C$ values are consistent with groundwater input; the mixolimnion DIC $\delta^{13}C$ values are influenced by dilution with surface-water inputs, loss of CO_2 to the atmosphere, and removal of more negative $\delta^{13}C$ value DIC by primary producers; and the monimolimnion DIC $\delta^{13}C$ values are increasingly negative with depth due to the remineralization of organic carbon in the water column and sediments.

The DIC $\delta^{13}C$ values in the chemocline reflect groundwater input similar to a sulfidic spring south of Chittenango, New York (DIC $\delta^{13}C$ of $-11.7‰$) and groundwater well values (DIC $\delta^{13}C$ of $-10‰$, Thompson et al. 1997). These observations are supported by previous work that indicated a significant groundwater contribution to FGL (Takahashi et al. 1968; Havig et al. 2015 and references therein). A groundwater DIC $\delta^{13}C$ value of close to $-12‰$ is expected from the reaction of aqueous CO_2 derived from the microbial respiration of organic carbon (producing H_2CO_3 with a $\delta^{13}C$ value of approximately $-25‰$) reacting with marine

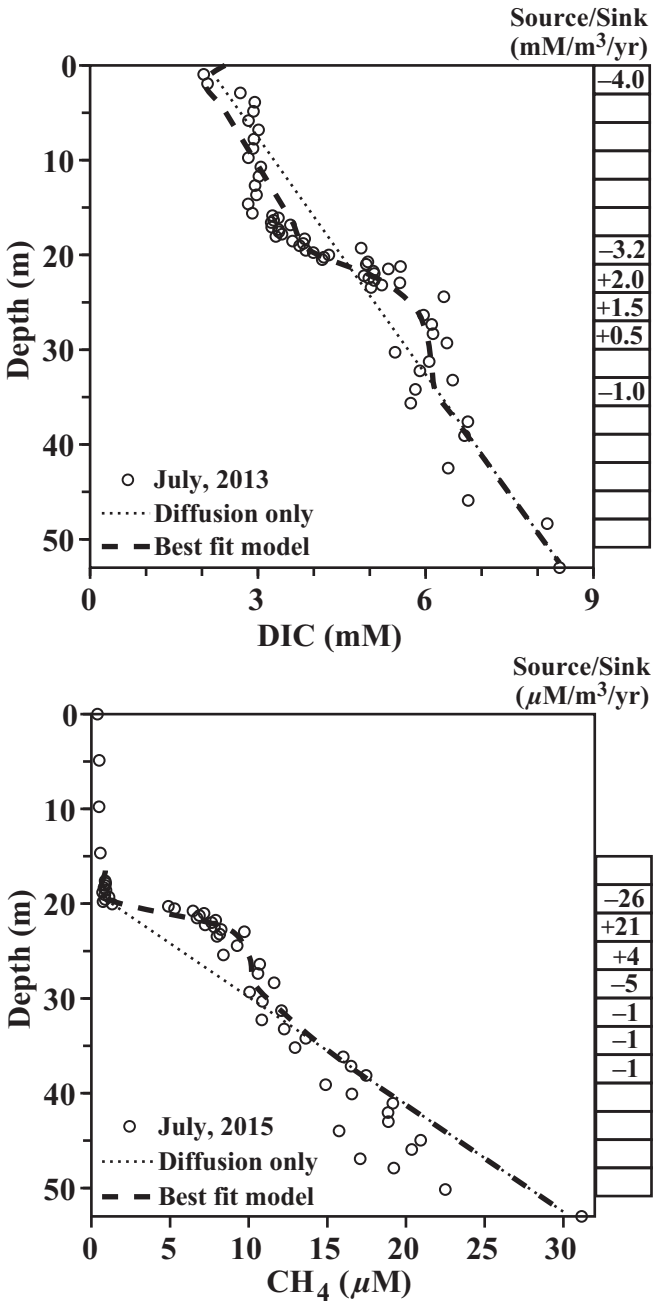

Fig. 8. 1D box model results for DIC (top) and CH_4 (bottom) showing data (open circles), model results for diffusion only (dotted line), and best fit model results incorporating diffusion, sources, and sinks (dashed line). Sources and sinks estimated via best fit modeling are indicated for each 3 m depth interval box are given on the right side of each plot, with units indicated at the top.

carbonate rock (with $CaCO_3$ with a $\delta^{13}C$ value of $\sim 0‰$, Deines et al. 1974). The mixolimnion DIC $\delta^{13}C$ values are influenced by dilution with surface-water inputs, loss of CO_2 to the atmosphere (Takahashi et al. 1968: this study, Supporting Information Material) leading to preferential loss of $^{12}CO_2$, and removal of more negative $\delta^{13}C$ value DIC by primary producers during carbon fixation. These processes drive mixolimnion DIC $\delta^{13}C$ values more positive. Monimolimnion DIC $\delta^{13}C$ values, on the other hand, are increasingly negative with depth due to the mineralization of organic carbon in the water column and sediments with $\delta^{13}C$ values of $-29‰$ to $-40‰$. Increasing DIC concentration with depth in the sediment pore water coupled to DIC $\delta^{13}C$ values reaching $-25.2‰$ (Fig. 6) indicate organic carbon mineralization is occurring in the sediments, likely due to fermentation and subsequent oxidation by sulfate reducing organisms (SROs) given the availability of sulfate and high concentration of sulfide in the sediments (Fig. 4). Other redox-coupled metabolisms (manganese reduction, iron reduction, nitrate reduction, etc.) are not likely to be significant below the redoxcline (Havig et al. 2015).

A simple 1D box diffusion model with 3-m layer spacing was constructed (integrated over 20 yr) to estimate possible sources and sinks of DIC in the water column (Fig. 8). Simple diffusion explained the overall trend in DIC concentration in the water column, but to explain the deviations from the diffusion line, sources, and sinks were required. Specifically, DIC sinks of 4 $mM/m^3/yr$ for the 0–3 m depth interval and of 3.2 $mM/m^3/yr$ for the 18–21 m interval are consistent with carbon fixation and precipitation of carbonate at the surface and within the bacterial plate at the base of the chemocline. Sources of DIC peak just below the chemocline (2 $mM/m^3/yr$ for the interval from 21 m to 24 m), then decline gradually (1.5 $mM/m^3/yr$ between 24 m and 27 m and 0.5 $mM/m^3/yr$ from 27 m to 30 m). These values are consistent with mineralization of organic carbon in the upper portions of the monimolimnion. While an additional DIC sink at the 33–36 m interval (1 $mM/m^3/yr$) may indicate carbon fixation, it might also reflect a second chemocline suggested previously (e.g., Jelacic 1970; Torgersen et al. 1981).

DOC $\delta^{13}C$ values show little variation through the water column, suggesting the DOC is likely recalcitrant organic carbon, and that labile DOC is rapidly cycled so that its influence on DOC $\delta^{13}C$ values is minimal (Fig. 5). DOC concentration is consistently at or below 200 μM and nearly unchanging through the water column, supporting this hypothesis. Sediment pore-water DOC concentrations are about an order of magnitude higher than in the water column, and have isotopic values that indicate input from chemocline and monimolimnion sourced biomass (e.g., seston), as well as potential input of isotopically light DOC from oxidation of CH_4.

Methane

Methane concentration increases below the chemocline ($\sim$ 20 m), reaching a maximum of $\sim$ 20 μM near 50 m (Fig. 5). Similarly, concentration of methane increases in the sediments to a maximum of 137.4 μM at 30 cm (Fig. 6). The

Table 1. Geochemistry of inputs to and outflow from FGL.

	Units	Sulfide spring	Round Lake OF	Green Lake OF
UTM	m	4762750	4766646	4767716
18T	m	0430840	0420851	0421627
Elevation	m	176	128	127
pH	—	7.2	7.7	8.0
Temperature	°C	11.2	22.9	24.4
Conductivity	μS/cm	2050	1879	1898
DIC	mmol/L	4.9	3.5	2.9
DIC	‰	−11.7	−8.1	−6.9
DOC	mmol/L	0.07	0.13	0.12
DOC	‰	−29.0	−27.7	−28.6
Chloride	mmol/L	1.45	—	—
Sulfate	mmol/L	15.84	—	—
Ammonium	μmol/L	571	—	—
Sodium	mmol/L	1.06	—	—
Calcium	mmol/L	14.42	—	—
Magnesium	mmol/L	3.82	—	—
Silicon	μmol/L	165	—	—

Conductivity adjusted to equivalent at 25°C. UTM = Universal Transverse Mercator, OF = outflow.

increase with depth into the sediments indicates a diffusion from a source below 30 cm. The shape of the methane concentration profile in the water column is similar to that reported by Torgersen et al. (1981), but differs from that of other stratified systems (Reeburgh et al. 2006; Dahl et al. 2010; Schubert et al. 2011) where methane concentrations typically increase dramatically below a redoxcline and then are constant throughout the lower water column. Diffusion of CH_4 from a sole sediment source would produce a straight line. However, a shoulder in the CH_4 concentration below the chemocline that then declines with depth is inconsistent with diffusion. Matching the concentration curve through construction of a simple 1D diffusion model over a 20 yr time interval allowed estimation of sources and sinks at different depths in the water column (Fig. 8). For CH_4, the best fit was obtained with CH_4 sources of 21 μmol CH_4/m^3/yr for 21–24 m and 4 μmol CH_4/m^3/yr for 24–27 m and sinks of 26 μmol CH_4/m^3/yr from 18 m to 21 m, 5 μmol CH_4/m^3/yr for 27–30 m and 1 μmol CH_4/m^3/yr between 30 m and 39 m (Fig. 8) suggesting methane production in the water column. However, we failed to amplify the gene (*mcr*) that encodes the alpha subunit of the methyl-coenzyme M reductase from water column samples collected from 20.5 m, 24 m, or 30 m. Furthermore, PCRs of genomic DNA (gDNA) extracted from the top 50 cm of sediment samples also failed to amplify *mcr*. Methyl-coenzyme M reductase is present in all methanogens and catalyzes the last step in methanogenesis. In addition, there was no measurable methane production in mesocosms from the same depths (see Supporting Information Material for details). These sources likely represent inputs of groundwater at around 20 m (Thompson et al. 1990) accelerating the diffusive upward flux toward the sink for methane within the chemocline.

A potential source for methane in FGL is from CH_4-bearing/generating sedimentary units. Based on water and gas analysis, the majority of methane at depth (> 168 m) in Devonian-aged shales and sandstones that are part of the northern Appalachian Basin margin is thermogenic in origin, with $\delta^{13}C$ values that range from −53.3‰ to −40.2‰ (Osborn and McIntosh 2010). However, small accumulations of biogenic CH_4 were detected at shallow depths in western New York, with $\delta^{13}C$ values that range from −74.7‰ to −57.9‰ (Osborn and McIntosh 2010). Groundwater wells in Arkansas underlain by CH_4-containing shales had CH_4 $\delta^{13}C$ values that ranged from biogenic (lowest CH_4 $\delta^{13}C$ value of −74.7‰) to thermogenic (highest CH_4 $\delta^{13}C$ value of −42.3‰) (Warner et al. 2013). If methane at FGL was from similar sources, we would expect to find values within these ranges.

Methane in water column samples is remarkably light, with $\delta^{13}C$ between −99.1‰ and −102.3‰, indicating a biogenic origin (Fig. 5). Methane $\delta^{13}C$ measured at a mixolimnion depth of 10 m was −66.2‰. This value is between the monimolimnion values (ca. −100‰) and that of atmospheric CH_4 (−47.1‰, Whiticar 1999), indicating mixing of the two sources. All of the values found at FGL can be attributed to a biotic source of methane—methanogenesis can produce fractionation factors of up to 77‰ (with methanol as the source for C, methyltrophic) and 58‰ (with CO_2 as the source of C, hydrogenotrophic) in pure culture experiments (Whiticar 1999). Typically, hydrogenotrophic methanogenesis produces the most negative $\delta^{13}C$ values and

greatest fractionations (up to 95‰) observed in natural systems (Whiticar 1999). Assuming the smallest possible fractionation (subtracting the most negative sediment pore-water δ^{13}C-DIC value of −25.2‰ from water column δ^{13}C-CH_4 values), fractionation factors are ca. 77‰, suggesting hydrogenotrophic methanogenesis as a potential source of methane in FGL. In Lago di Cadagno, a permanently stratified lake in the Swiss Alps, the δ^{13}C fractionation factors for sediment CH_4 from DIC (data from Schubert et al. 2011) are up to 77‰, similar to those estimated for FGL. Methane is produced in the upper 30 cm of sediments in Lago di Cadagno due in part to drawdown of sulfate to values less than 100 μM by the action of SROs. In contrast, this extreme drawdown of sulfate was not observed in the top 48 cm of sediment in FGL (Fig. 4). An alternative hypothesis for the generation of negative CH_4 δ^{13}C values comes from isotopic fractionation effects in adsorption/desorption systems during mass transport of thermogenically produced CH_4 through rocks and sediments. While laboratory experiments indicate that the fractionations can be great, extrapolation to geologic processes predict a maximum change of only ∼ 5‰ more negative from the original value (Xia and Tang 2012). This is supported by the lack of extremely negative values from natural sources in the region (e.g., Osborn and McIntosh 2010; Osborn et al. 2011) or other natural gas producing regions (e.g., Warner et al. 2013).

The methane δ^{13}C values measured in the monimolimnion water column at FGL were most similar to those reported from sediment core pore-water analyses for samples collected from the Orca Basin in the Gulf of Mexico (lowest CH_4 δ^{13}C value of −105‰, Sackett et al. 1979) and the King George Basin of Antarctica (lowest CH_4 δ^{13}C value of −101.9‰, Whiticar and Suess 1990). The conditions in both basins are similar to those predicted to favor the co-occurrence of SROs and methanogens (Mitterer 2010). Traditionally sulfate reduction and methanogenesis have been viewed as competitive metabolic pathways, with SROs out-competing methanogens for energetic substrates (e.g., H_2, acetate). However, methylotrophic methanogens produce CH_4 via the breakdown of noncompetitive methylated substrates such as methanol ($4\ CH_3OH \rightarrow 3\ CH_4 + CO_2 + 2\ H_2O$), trimenthyl amine ($4\ (CH_3)_3N + 6\ H_2O \rightarrow 9\ CH_4 + 3\ CO_2 + 4\ NH_3$), and dimethylsulfide ($2\ (CH_3)_2S + 2\ H_2O \rightarrow 3\ CH_4 + CO_2 + 2\ H_2S$), allowing production of CH_4 in zones of active sulfate reduction by SROs. The co-occurrence of sulfate reduction and methane production in marine sediments has been documented where (1) there are noncompetitive substrates available to methanogens and SROs, (2) there is moderate to high total organic carbon present, (3) there is a source of sulfate in the sediment sub-seafloor (e.g., brine), (4) there is a moderate to high sedimentation rate, and (5) the sediments are carbonate-dominant (Mitterer 2010). FGL sediments have characteristics which are consistent with the co-occurrence of SROs and methanogens: high organic carbon content (Fig. 6), sulfate in the pore water (Fig. 4) possibly from a deeper brine source (Brunskill and Harriss 1969), a sedimentation rate of 0.1–0.7 mm/yr (Hilfinger et al. 2001), and carbonate-dominant lithology (Hilfinger et al. 2001; Fig. 6). A study of sediments from the Orca Basin (a hypersaline submarine environment sulfate concentrations ca. 40 mM) indicated methylotrophic methanogenesis was the source of CH_4 with δ^{13}C values of −77‰ to −89‰ (Zhuang et al. 2016). Pure culture experiments have indicated methylotrophic methanogenesis can produce extremely isotopically light CH_4. In one study, *Methanosarcina barkeri* generated CH_4 with δ^{13}C values of −112.2‰ to −114.2‰ from a methanol substrate with δ^{13}C values of −39.9‰ (Krzycki et al. 1987). In another study, *Methanococcoides burtonii* generated CH_4 with a δ^{13}C value of −97‰ from a trimethyl amine substrate with δ^{13}C values of −36.9‰ (Summons et al. 1998). These values are consistent with more recent work reporting fractionation factors of −72‰ to −83‰ generating CH_4 with δ^{13}C values at or below −100‰ from a methanol substrate for pure cultures of *Methanosarcina barkeri*, *Methanosarcina acetivorans*, and *Methanolobus zinderi* (Penger et al. 2012). While fractionation and absolute δ^{13}C values of CH_4 generated via methylotrophic methanogenesis in natural systems is still poorly constrained, the environmental conditions in FGL pore water suggest extremely negative δ^{13}C CH_4 found in the water column is likely sourced from this pathway. Given the results of our 1D model, we propose CH_4 is being generated primarily in the sediments and diffusing into the water column, with an input of CH_4 associated with lateral groundwater input.

Sediment carbonate

Carbonate minerals are the dominant mineralogy of FGL sediments (due to cyanobacteria *Synechococcus* spp. driving calcite precipitation in the water column, as described in Thompson et al. 1997), with greater wt. % $CaCO_3$ values below 20 cm (86–89%), and lower wt. % $CaCO_3$ values across the 20 cm transition (73%) which then increase to values that approach those of the deep sediments at the surface (82%) (Fig. 6). Cores collected at FGL (47 cm total sediment depth) from a previous study were dated to ∼ 2500 yr before present based on varve counting coupled to ^{14}C dating of plant material (Hilfinger et al. 2001). Previous work has shown that carbonate below the ∼ 20 cm transition is calcite, while above the transition there is a significant input of dolomite from the accelerated erosion of local bedrock by deforestation and agriculture following European settlement of the area ca. 1770 CE (Hilfinger et al. 2001). Through this transition, the size of calcite crystals in the deeper sediments is significantly larger than those found above the transition (Fig. 7). From counts conducted on SEM images, 59% of crystals had a long axis that fell between 4 μm and 8 μm for the 0–5 cm depth range (average of 7.4 μm), while 58% of crystals had a long axis that fell between 6 μm and 12 μm for

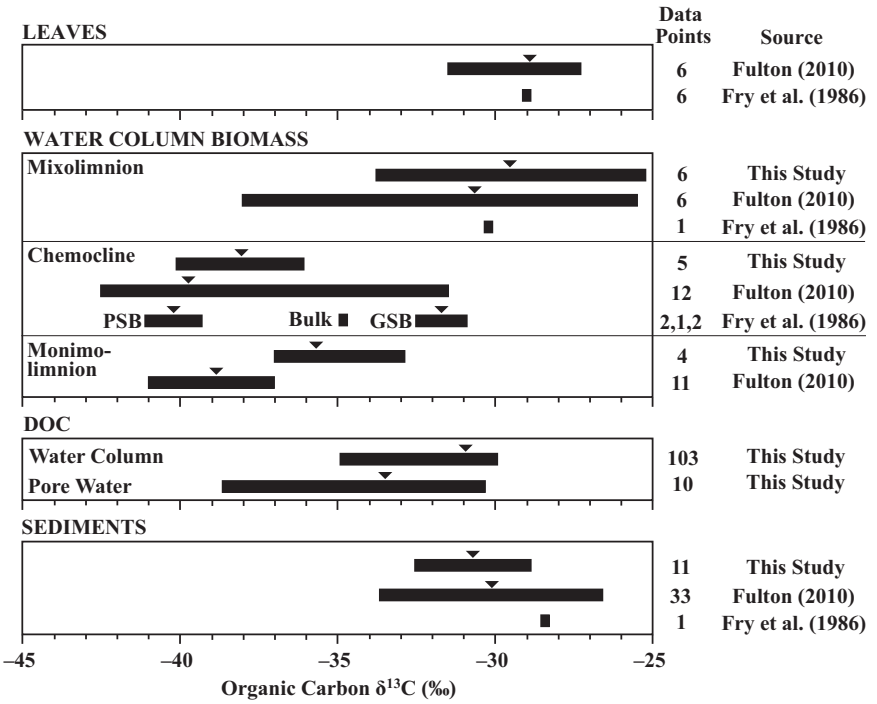

Fig. 9. Organic carbon stable isotope data associated with FGL, New York, including allochthonous plant material (leaves), autochthonous biomass (water column), water column DOC, and sediment organic carbon (sediments). Data from Fry (1986), Fulton (2010), and this study. Black horizontal bar encompasses full data range, with a triangle indicating mean values when there is more than one data point, and number of data points given. All carbon isotope values are reported vs. VPDB standard, in units of per mil (‰).

the 40–48 cm depth range (average of 10.3 μm). The decrease in calcite crystal size observed between the deep and surface sediments at FGL may reflect a decrease in calcite precipitation rates as a result of increasing pCO_2 in the atmosphere from anthropogenic sources, resulting in acidification lowering calcite saturation indices (which would have been further compounded by release of NO_x and SO_2 from the burning of coal producing HNO_3 and H_2SO_4). An alternate hypothesis is that more recent whiting events (precipitation of carbonate minerals in the water column, resulting in a milky appearance) have become more dense, resulting in a shorter period of crystal growth before settling. Precipitation of carbonate with increasing depth leading to coarsening crystal size is inconsistent with the carbonate $\delta^{13}C$ values found in the FGL sediments (Fig. 6 and described below).

Carbonate $\delta^{13}C$ values in the sediments have an average value of $-4.3‰$, and fall within a tight range ($-4.2‰$ to $-5.0‰$) (Fig. 6), similar to values reported in previous studies (Takahashi et al. 1968; Fry 1986; Thompson et al. 1997; Hilfinger et al. 2001; Fulton 2010). Sediment carbonate $\delta^{13}C$ values are similar to those measured for carbonates filtered from water depths of 0 m ($-5.4‰$) and 10 m ($-5.5‰$), and values for carbonates measured from surface water and thrombolite material reported in Thompson et al. (1997). This similarity between carbonates precipitating in the oxic zone to those deposited over the last $\sim$ 2500 yr (represented by the sediment core) suggest water column precipitation is the primary source of carbonate minerals in the sediments.

Sediment organic carbon

Sediment organic carbon ranges from 1.8% to 4.2% making it a sapropel, which is consistent with euxinic conditions acting to inhibit organic carbon oxidation and loss (Fig. 6). Lower values in the upper sediments may partially be the result of dilution with increased inorganic detrital sedimentation, though there is no abrupt shift near 20 cm. Organic carbon $\delta^{13}C$ values were $-32.6‰$ for the 40–48 cm depth interval, and increased slightly to values between $-32‰$ and $-31‰$ from 25 cm to 40 cm, then exhibited a further increase to a high of $-29.0‰$ to $-28.8‰$ for sediments between 10 cm and 20 cm before dropping back down to $-32.6‰$ at the surface (equal to those of the deepest sediments) (Fig. 6). These organic carbon $\delta^{13}C$ values indicate greater input of organic carbon from sources with more negative $\delta^{13}C$ organic carbon in the deeper sediments (below 25 cm) and at the surface (0–5 cm), and a more positive $\delta^{13}C$ organic carbon source between 5 cm and 25 cm (peaking between 10 cm and 20 cm). A source of more negative $\delta^{13}C$ organic carbon includes primary productivity by PSB and GSB at and below 20 m, with seston $\delta^{13}C$ values that range from $-37‰$ and $-42‰$ (Table 1; Fig. 9). Note that GSB use the reverse tricarboxylic acid (rTCA) pathway for fixing carbon, which typically yields relatively smaller fractionations

(Havig et al. 2011 and references therein), however GSB are also capable of uptake and incorporation of organic compounds in conjunction with autotrophic photosynthesis (Fuchs et al. 1980), which could be generated by fermenters from PSB-sourced organic material. More positive organic carbon $\delta^{13}C$ values may be sourced from higher plant material (e.g., tree leaves, with a range of −27.3‰ to −31.5‰) or from primary productivity in the upper 10 m of the water column where seston can have values of between −25.5‰ and −33.0‰ (Fig. 9; Fulton 2010). Assuming no preferential breakdown of organic matter across the 48 cm sediment depth range, organic carbon $\delta^{13}C$ values may reflect a relative decrease in more negative organic carbon and an increase in less negative organic carbon between 5 cm and 25 cm depths. An alternative would be an increased rate of breakdown of isotopically lighter organic matter between 5 cm and 25 cm leaving heavier recalcitrant organic matter behind; though this is not reflected in the total organic carbon values (Fig. 9). Pore-water DOC $\delta^{13}C$ values from 0 cm to 10 cm are approximately 1.5–2‰ more negative than sediment organic C, and below 20 cm are approximately 2.8–2.9‰ more negative, and are from 3.3‰ to 10.0‰ more negative between 10 cm and 20 cm (Fig. 6). Our first order assumption is that the DOC is produced from the breakdown of labile microbial biomass, while sediment organic C is a combination of more recalcitrant allochthonous plant and soil material and autochthonous microbial biomass. The positive trend in sediment organic carbon $\delta^{13}C$ values above 20 cm is consistent with greater influence of more positive soil and/or plant material input following European settlement of the FGL area, while the sharp shift of DOC $\delta^{13}C$ for the 16–19 cm depth range to more negative (and similar to PSB biomass values ca. 40‰) indicates a concurrent shift toward a greater influence of PSB on DOC. It is important to note that the sedimentation rate at FGL increased by seven times with the onset of European settlement (Hilfinger et al. 2001), so adjusting the % organic C content indicates the amount of organic carbon being deposited in FGL sediments increased dramatically, with an adjusted value of 22.0% organic carbon for the 10–20 cm depth range, 15.7% for 5–10 cm, and 12.6% for 0–5 cm. Thus, it appears that there was an increase in biomass being delivered to the sediments in FGL concurrent with European settlement and shift toward agricultural land use around FGL. The subsequent negative shift of $\delta^{13}C$ values for carbonate minerals as well as organic carbon in the uppermost sediments coincides with the onset of fossil fuel burning associated with the industrial revolution (12 cm depth ≈ the year 1850, Hilfinger et al. 2001). The increasing use of fossil fuels since that time has resulted in a shift of atmospheric CO_2 $\delta^{13}C$ values from approximately −6.5‰ circa the year 1850 (Friedli et al. 1986) to modern values of approximately −8.3‰ circa the year 2013 (United States Department of Energy), and this change could help explain the shift to more negative $\delta^{13}C$ values in the uppermost sediments at FGL.

Carbon isotope conceptual model

Modern redox-stratified water bodies such as FGL may serve as useful proxies to elucidate the effects of stratification on inorganic and organic carbon burial and resulting carbon isotope signals transferred to the rock record. A conceptual 1D model interpreting the results of analyses of water column and sediment samples collected at FGL illustrates the primary influences driving carbon isotopic values for inorganic and organic carbon (Fig. 10). All isotopic values are expressed as average $\delta^{13}C$ values, with any data included from previous studies indicated.

DIC $\delta^{13}C$ values within the chemocline reflect input of groundwater replete with DIC into FGL, consistent with what has been suggested previously (Deevey et al. 1963; Takahashi et al. 1968; Torgersen et al. 1981; Thompson et al. 1990; Havig et al. 2015). DIC $\delta^{13}C$ values are increased by approximately +4‰ in the mixolimnion relative to the groundwater input due to preferential removal of low $\delta^{13}C$ inorganic carbon through carbon fixation by diatoms and cyanobacteria (reflected as the DIC sink in Fig. 8). Loss of CO_2 to the atmosphere may also contribute to surface water with heavier $\delta^{13}C$ values through exchange at the surface and subsequent mixing (consistent with calculated *p*CO2 values greater than atmospheric values, Supporting Information Material), as well as precipitation input of DIC with values close to zero (in equilibrium with atmospheric CO_2). Inputs of organic carbon include biomass generated through carbon fixation by terrestrial plants, diatoms, cyanobacteria, PSB, and GSB. Primary productivity in the water column acts to preferentially transfer ^{12}C to the deeper water and sediments. Remineralization of organic carbon is driven by heterotrophic microorganisms (including SROs, fermenters, and methanogens) converting ^{12}C enriched organic carbon into DIC, thereby increasing the DIC pool concentration and making it more ^{12}C enriched. DIC in the monimolimnion is approximately −3‰ relative to groundwater DIC input from 21 m to 37 m, approximately −7‰ from 37 m to 53 m, and approximately −11‰ for sediment pore water, likely reflecting a diffusive gradient from remineralization of organic C in the sediments with additional water column remineralization occurring below the chemocline (Fig. 8).

Carbonate precipitation in the mixolimnion driven by cyanobacteria (esp. *Synechococcus* sp., Thompson et al. 1997) produces calcite that is heavier than the water DIC values, and that signal is transferred to the sediments. The fractionation between mixolimnion DIC $\delta^{13}C$ values and those of precipitated calcite is approximately +2‰, and the fractionation from the original groundwater DIC value is approximately +6‰. This carbonate is transferred to the sediments, and the $\delta^{13}C$ value remains essentially unaltered

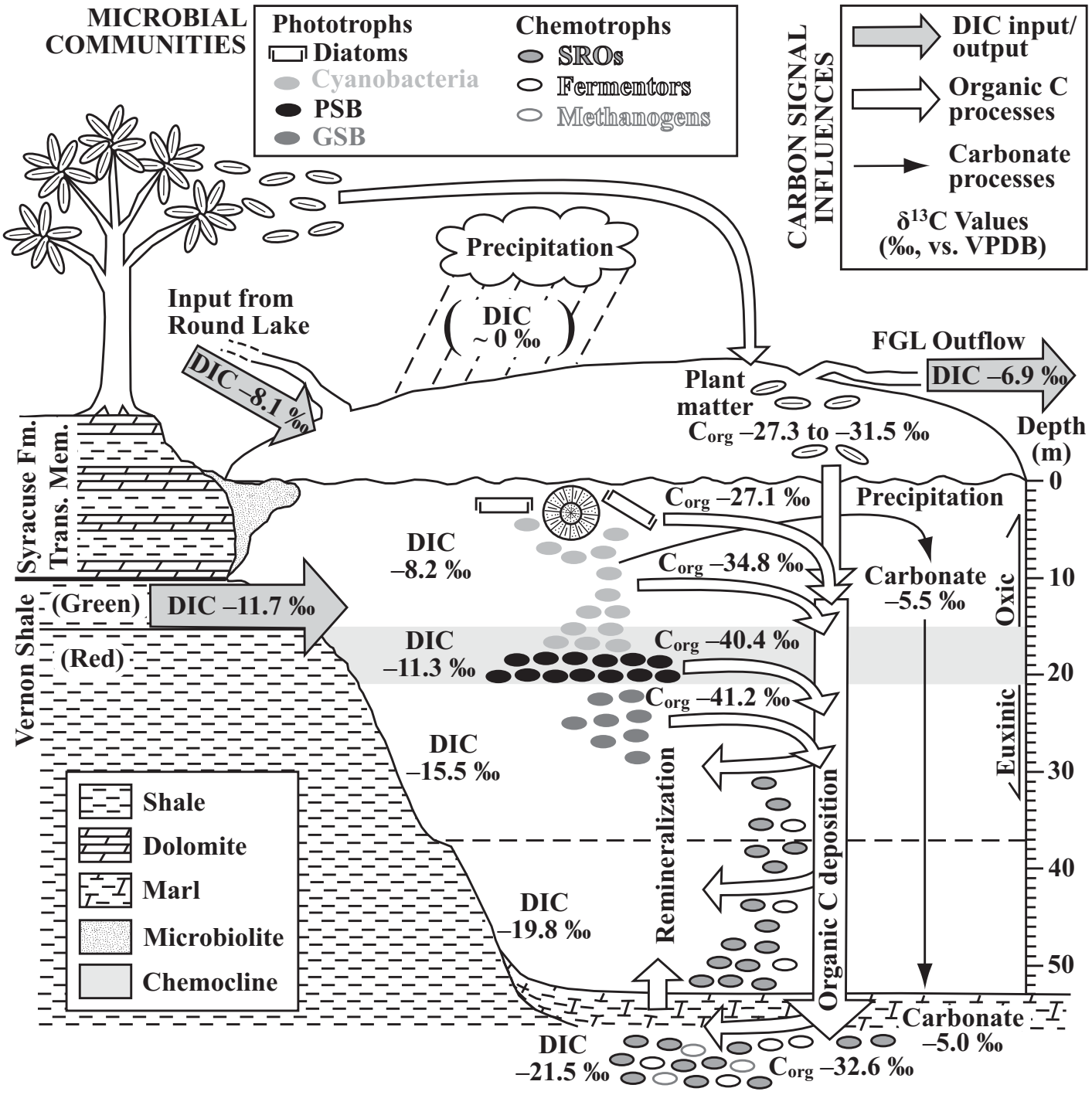

Fig. 10. Conceptual model for carbon cycling and resulting stable isotope signals at FGL. All water $\delta^{13}C$ values represent average values for the representative water layers. C_{org}, organic carbon; DIC, dissolved inorganic carbon; GSB, green sulfur bacteria; PSB, purple sulfur bacteria; SROs, sulfate reducing organisms. Sediment values represent surface (0–5 cm depth range). Plant matter values are from leaf biomass analyses in Fulton (2010). Water column C_{org} values calculated using data from this study and Fulton (2010).

in spite of the high concentration of ^{12}C enriched DIC (average of 10.4 mM) as well as calcium (average of 14.1 mM) in the sediment pore water maintaining calcite super-saturation.

Relevance of FGL for systems with increasing anoxia

Increasing temperatures due to global climate change are predicted to lead to higher lake surface temperatures that will increase thermal stratification and stability (Einsele et al.

2001; Ficke et al. 2007). Furthermore, higher surface temperatures will lead to increased cyanobacterial and algal biomass production which will drive increasing anoxia in deeper water due to increasing organic carbon oxidation of that produced biomass as well as associated carbonate precipitation (Einsele et al. 2001; Ficke et al. 2007). Supporting this, a study of the effects of the 2003 summer heat wave in Europe on two Swiss lakes showed an increase in overall thermal stratification and stability, and dissolved oxygen depletion in the hypolimnions of both (Jankowski et al. 2006). Using FGL as a perennially stratified end-member for the effects of increasing anoxia in lakes and reservoirs, we can make predictions for the effects on carbon cycling and sequestration. While it has long been established that anoxic conditions are advantageous to sequestration of organic carbon in sediments (e.g., Canfield 1994), precipitation of carbonate in the water column can also be an important sink for carbon in lakes. At FGL (owing to the high calcium concentrations), the sediments sequester 2–6 times as much C as carbonate (8.8–10.6% C dry weight in sediments) then as organic carbon (1.8–4.2% C dry weight in sediments). Also, heterotrophic breakdown of organic C and conversion into DIC leads to large amounts of C in the water column (Fig. 5) as well as sediment pore water (Fig. 6). Longer periods of thermal stratification coupled to increased productivity by benthic photoautotrophs may lead to an increase in the amount of organic carbon sequestered in sediments, though this might also drive increased methanogenesis (e.g., Waseda 1998). Increased occurrence and length of cyanobacterial bloom periods in lakes where carbonate precipitation occurs in the water column as a result will also lead to increased sequestration of C in the sediments. Increased occurrences of thermal and redox stratification may also lead to an increased roll for anoxygenic photosynthesis in primary productivity in lakes where the redox transition occurs in the photic zone. Overall, the impacts of increased stratification in lakes on the local and global carbon cycle will depend on the physical and geochemical conditions of the lake in question.

Potential perspectives for the paleoproterozoic ocean

The effects of the oxic/euxinic redox stratification of FGL may serve as a model for similar conditions that occurred in the oceans during the Paleoproterozoic. One is the large role carbonate precipitation in the water column plays in carbon sequestration into the sediments at FGL, where most of the precipitation occurs in the upper oxic mixolimnion. Another is the large range of DIC concentration and $\delta^{13}C$ values for DIC from the oxic mixolimnion through to the euxinic monimolimnion and on into the sediment pore water (Figs. 5, 6). Owing to heterotrophic breakdown of organic material generating DIC, there is an increase in concentration by a factor of two in the mixolimnion and four in the sediment pore water compared to the mixolimnion. Mirroring this increase in concentration is a decrease in the DIC $\delta^{13}C$ values of $-12‰$ in the monimolimnion and $-16‰$ in the sediment pore water vs. the mixolimnion. If global circulation patterns were to stagnate for a significant period of time, this could lead to an increase in the amount of DIC stored in the deep ocean. A further effect is the relatively high DOC concentration in the monimolimnion (70–262 μmol/L) observed at FGL (Fig. 6). These values may prove useful as estimates for global ocean C cycling models for redox stratified oceans, especially given they range from similar to, to much higher than the highest values for the modern ocean (Hansell 2013). Last, the generation of CH_4 in FGL sediments with extremely negative $\delta^{13}C$ values ($-99.1‰$ to -102.3 ‰) in the presence of high sulfate concentrations may have implications for the generation of methanotrophic biomass with anomalously negative biomass $\delta^{13}C$ values (i.e., the Francevillian excursion circa 2.0 Ga, Schidlowski 2001) without the need for sulfate concentrations to decrease enough to limit SROs.

Conclusions

Investigation and high depth-resolution sampling of the water column and sediments at FGL have revealed a complex carbon cycle resulting in unique inorganic and organic carbon stable isotope signals. The groundwater input with high concentrations of calcium, sulfate, and bicarbonate maintains the meromictic nature of FGL where primary productivity is driven by different communities in the upper water column and sulfate reducing bacteria produce sulfide to sustain euxinia below 21 m. Carbon fixation and concurrent calcite precipitation decrease the DIC concentration in the upper 15 m of the FGL water column and drive DIC $\delta^{13}C$ values positive by approximately $+4‰$ (relative to the groundwater input) resulting in precipitation of calcite that is enriched by approximately $+6‰$ relative to the input source (groundwater DIC). As a result of remineralization of organic matter, DIC concentration increases with depth below the chemocline ($>$ 21 m depth), and DIC $\delta^{13}C$ values become enriched in ^{12}C driving deep DIC $\delta^{13}C$ values to approximately $-7‰$ (relative to groundwater input). Possible noncompetitive co-occurrence of sulfate reducing bacteria and methanogens allows for the production of methane in spite of copious amounts of sulfate present in the sediments, generating methane with $\delta^{13}C$ values of $-99.1‰$ to $-102.3‰$ (the most negative values yet recorded for a nonmarine system, and only the third report of natural abundance $\delta^{13}C$ values below $-100‰$ known to the authors).

Our data indicate complex carbon cycling in a permanently stratified lake which is distinct from other systems and underscore the need for future studies in other stratified systems. FGL and other stratified systems can serve as valuable end-members for understanding the role of increasing occurrences of thermal and redox stratification in lakes and reservoirs on global carbon cycling. Similarly, these redox-

stratified systems are valuable analogs of carbon cycling in the oceans during the Paleoproterozoic (as well as other times of global ocean redox stratification).

References

Anderson, N. J., R. D. Dietz, and D. R. Engstrom. 2013. Land-use change, not climate, controls organic carbon burial in lakes. Proc. R. Soc. B **280**: 20131278. doi:10.1098/rspb.2013.1278

Anderson, N. J., H. Bennion, and A. F. Lotter. 2014. Lake eutrophication and its implications for organic carbon sequestration in Europe. Glob. Chang. Biol. **20**: 2741–2751. doi:10.1111/gcb.12584

Brunskill, G. J., and R. C. Harriss. 1969. Fayetteville Green Lake, IV. Interstitial water chemistry of the sediments. Limnol. Oceanogr. **14**: 858–861. doi:10.4319/lo.1969.14.6.0858

Brunskill, G. J., and S. D. Ludlam. 1969. Fayetteville Green Lake, New York. I. Physical and chemical limnology. Limnol. Oceanogr. **14**: 817–829. doi:10.4319/lo.1969.14.6.0817

Canfield, D. E. 1994. Factors influencing organic carbon preservation in marine sediments. Chem. Geol. **114**: 315–329. doi:10.1016/0009-2541(94)90061-2

Dahl, T. W., A. D. Anbar, G. W. Gordon, M. T. Rosing, R. Frei, and D. E. Canfield. 2010. The behavior of molybdenum and its isotopes across the chemocline and in the sediments of sulfidic Lake Cadagno, Switzerland. Geochim. Cosmochim. Acta **74**: 144–163. doi:10.1016/j.gca.2009.09.018

Deevey, E. S., N. Nakai, and M. Stuiver. 1963. Fractionation of sulfur and carbon isotopes in a meromictic lake. Science **139**: 407–407. doi:10.1126/science.139.3553.407

Deines, P., D. Langmuir, and R. S. Harmon. 1974. Stable carbon isotope ratios and the existence of a gas phase in the evolution of carbonate ground waters. Geochim. Cosmochim. Acta **38**: 1147–1164. doi:10.1016/0016-7037(74)90010-6

Dong, X., N. J. Anderson, X. Yang, X. Chen, and J. Shen. 2012. Carbon burial by shallow lakes on the Yangtze floodplain and its relevance to regional carbon sequestration. Glob. Chang. Biol. **18**: 2205–2217. doi:10.1111/j.1365-2486.2012.02697.x

Downing, J. A., J. J. Cole, J. J. Middelburg, R. G. Striegl, C. M. Duarte, P. Kortelainen, Y. T. Prairie, and K. A. Laube. 2008. Sediment organic carbon burial in agriculturally eutrophic impoundments over the last century. Global Biogeochem. Cycles **22**: GB1018. doi:10.1029/2006GB002854

Eggleton, F. E. 1931. A limnological study of the profundal bottom fauna of certain fresh-water lakes. Ecol. Monogr. **1**: 231–331. doi:10.2307/1943114

Eggleton, F. E. 1956. Limnology of a meromictic, interglacial, plunge-basin lake. Trans. Am. Microsc. Soc. **75**: 334–378. doi:10.2307/3223965

Einsele, G., J. Yan, and M. Hinderer. 2001. Atmospheric carbon burial in modern lake basins and its significance for the global carbon budget. Glob. Planet. Change **30**: 167–195. doi:10.1016/S0921-8181(01)00105-9

Ficke, A. D., C. A. Myrick, and L. J. Hansen. 2007. Potential impacts of global climate change on freshwater fisheries. Rev. Fish Biol. Fish. **17**: 581–613. doi:10.1007/s11160-007-9059-5

Friedli, H., H. Lötscher, H. Oeschger, U. Siegenthaler, and B. Stauffer. 1986. Ice core record of the C-13/C-12 ratio of atmospheric CO_2 in the past two centuries. Nature **324**: 237. doi:10.1038/324237a0

Fry, B. 1986. Sources of carbon and sulfur nutrition for consumers in three meromictic lakes of New York State. Limnol. Oceanogr. **31**: 79–88. doi:10.4319/lo.1986.31.1.0079

Fry, B., and E. B. Sherr. 1989. $\delta^{13}C$ measurements as indicators of carbon flow in marine and freshwater ecosystems, p. 196–229. *In* P. W. Rundel, J. R. Ehleringer, K. A. Nagy (Eds.), Stable isotopes in ecological research. Springer, New York, NY.

Fuchs, G., E. Stupperich, and G. Eden. 1980. Autotrophic CO2 fixation in *Chlorobium limicola*. Evidence for the operation of a reductive tricarboxylic acid cycle in growing cells. Arch. Microbiol. **128**: 64–71. doi:10.1007/BF00422307

Fulton, J. M. 2010. Interpreting nitrogen isotope excursions in the sedimentary record. Unpubl. Ph.D. thesis. The Pennsylvania State Univ.

Hansell, D. A. 2013. Recalcitrant dissolved organic carbon fractions. Ann. Rev. Mar. Sci. **5**: 421–445. doi:10.1146/annurev-marine-120710-100757

Havig, J. R., J. Raymond, D. A. R. Meyer-Dombard, N. Zolotova, and E. L. Shock. 2011. Merging isotopes and community genomics in a siliceous sinter-depositing hot spring. Journal of Geophysical Research: Biogeosciences **116**(G1). doi:10.1029/2010JG001415

Havig, J. R., M. L. McCormick, T. L. Hamilton, and L. R. Kump. 2015. The behavior of biologically important trace elements across the oxic/euxinic transition of meromictic Fayetteville Green Lake, New York, USA. Geochim. Cosmochim. Acta **165**: 389–406. doi:10.1016/j.gca.2015.06.024

Heathcote, A. J., and J. A. Downing. 2012. Impacts of eutrophication on carbon burial in freshwater lakes in an intensively agricultural landscape. Ecosystems **15**: 60. doi:10.1007/s10021-011-9488-9

Hilfinger IV, M. F., H. T. Mullins, A. Burnett, and M. E. Kirby. 2001. A 2500 year sediment record from Fayetteville Green Lake, New York: Evidence for anthropogenic impacts and historic isotope shift. J. Paleolimnol. **26**: 293–305. doi:10.1023/A:1017560300681

Hunter, S. E. 2012. Spatio-temporal variability in the phototrophic chemocline community at Fayetteville Green Lake (New York). Unpubl. M.S. thesis. The Pennsylvania State Univ.

Jankowski, T., D. M. Livingstone, H. Bührer, R. Forster, and P. Niederhauser. 2006. Consequences of the 2003 European heat wave for lake temperature profiles, thermal

stability, and hypolimnetic oxygen depletion: Implications for a warmer world. Limnol. Oceanogr. **51**: 815–819. doi:10.4319/lo.2006.51.2.0815

Jelacic, A. J. 1970. Physical limnology of Green and Round Lakes. Fayetteville, New York. Unpubl. Ph.D. thesis. Univ. of Rochester.

Kastowski, M., M. Hinderer, and A. Vecsei. 2011. Long-term carbon burial in European lakes: Analysis and estimate. Global Biogeochem. Cycles **25**: GB3019. doi:10.1029/2010GB003874

Kritzberg, E. S., J. J. Cole Jonathan, M. L. Pace, W. Granéli, and D. L. Bade. 2004. Autochthonous versus allochthonous carbon sources of bacteria: Results from whole-lake 13C addition experiments. Limnol. Oceanogr. **49**: 588–596. doi:10.4319/lo.2004.49.2.0588

Krzycki, J. A., W. R. Kenealy, M. J. DeNiro, and J. G. Zeikus. 1987. Stable carbon isotope fractionation by *Methanosarcina barkeri* during methanogenesis from acetate, methanol, or carbon dioxide-hydrogen. Appl. Environ. Microbiol. **53**: 2597–2599.

McCormick, M. L., N. Banishki, S. Powell, A. Rumack, and J. M. Garrett. 2014. A low cost multi-level sampling device for synchronous aseptic collection of environmental water samples. J. Microbiol. Methods **105**: 51–53. doi:10.1016/j.mimet.2014.07.014

Meyer, K. M., and L. R. Kump. 2008. Oceanic euxinia in Earth history: Causes and consequences. Annu. Rev. Earth Planet. Sci. **36**: 251–288. doi:10.1146/annurev.earth.36.031207.124256

Mitterer, R. M. 2010. Methanogenesis and sulfate reduction in marine sediments: A new model. Earth Planet. Sci. Lett. **295**: 358–366. doi:10.1016/j.epsl.2010.04.009

Muller, E. H. 1967. Geologic setting of Green and Round Lakes near Fayetteville, New York, p. 96–121. *In* Some aspects of Meromixis. Department of Civil Engineering, Syracuse Univ.

Osborn, S. G., and J. C. McIntosh. 2010. Chemical and isotopic tracers of the contribution of microbial gas in Devonian organic-rich shales and reservoir sandstones, northern Appalachian Basin. Appl. Geochem. **25**: 456–471. doi:10.1016/j.apgeochem.2010.01.001

Osborn, S. G., A. Vengosh, N. R. Warner, and R. B. Jackson. 2011. Methane contamination of drinking water accompanying gas-well drilling and hydraulic fracturing. Proc. Natl. Acad. Sci. USA. **108**: 8172–8176. doi:10.1073/pnas.1100682108

Paerl, H. W., and J. Huisman. 2009. Climate change: A catalyst for global expansion of harmful cyanobacterial blooms. Environ. Microbiol. Rep. **1**: 27–37. doi:10.1111/j.1758-2229.2008.00004.x

Penger, J., R. Conrad, and M. Blaser. 2012. Stable carbon isotope fractionation by methylotrophic methanogenic archaea. Appl. Environ. Microbiol. **78**: 7596–7602. doi:10.1128/AEM.01773-12

Reeburgh, W. S., S. C. Tyler, and J. Carroll. 2006. Stable carbon and hydrogen isotope measurements on Black Sea water-column methane. Deep-Sea Res. Part II Top. Stud. Oceanogr. **53**: 1893–1900. doi:10.1016/j.dsr2.2006.03.018

Sackett, W. M., J. M. Brooks, B. B. Bernard, C. R. Schwab, H. Chung, and R. A. Parker. 1979. A carbon inventory for Orca Basin brines and sediments. Earth Planet. Sci. Lett. **44**: 73–81. doi:10.1016/0012-821X(79)90009-8

Schidlowski, M. 2001. Carbon isotopes as biogeochemical recorders of life over 3.8 Ga of Earth history: Evolution of a concept. Precambrian Res. **106**: 117–134. doi:10.1016/S0301-9268(00)00128-5

Schindler, D. E., S. R. Carpenter, J. J. Cole, J. F. Kitchell, and M. L. Pace. 1997. Influence of food web structure on carbon exchange between lakes and the atmosphere. Science **277**: 248–251. doi:10.1126/science.277.5323.248

Schubert, C. J., F. Vazquez, T. Lösekann-Behrens, K. Knittel, M. Tonolla, and A. Boetius. 2011. Evidence for anaerobic oxidation of methane in sediments of a freshwater system (Lago di Cadagno). FEMS Microbiol. Ecol. **76**: 26–38. doi:10.1111/j.1574-6941.2010.01036.x

Summons, R. E., P. D. Franzmann, and P. D. Nichols. 1998. Carbon isotopic fractionation associated with methylotrophic methanogenesis. Org. Geochem. **28**: 465–475. doi:10.1016/S0146-6380(98)00011-4

Takahashi, T., W. Broecker, Y. H. Li, and D. Thurber. 1968. Chemical and isotopic balances for a meromictic lake. Limnol. Oceanogr. **13**: 272–292. doi:10.4319/lo.1968.13.2.0272

Thompson, J. B., F. G. Ferris, and D. A. Smith. 1990. Geomicrobiology and sedimentology of the mixolimnion and chemocline in Fayetteville Green Lake, New York. Palaios **5**: 52–75. doi:10.2307/3514996

Thompson, J. B., S. Schultze-Lam, T. J. Beveridge, and D. J. Des Marais. 1997. Whiting events: Biogenic origin due to the photosynthetic activity of cyanobacterial picoplankton. Limnol. Oceanogr. **42**: 133–141. doi:10.4319/lo.1997.42.1.0133

Torgersen, T., D. E. Hammond, W. B. Clarke, and T. H. Peng. 1981. Fayetteville, Green Lake, New York: 3H-3He water mass ages and secondary chemical structure. Limnol. Oceanogr. **26**: 110–122. doi:10.4319/lo.1981.26.1.0110

Tranvik, L. J., and others. 2009. Lakes and reservoirs as regulators of carbon cycling and climate. Limnol. Oceanogr. **54**: 2298–2314. doi:10.4319/lo.2009.54.6_part_2.2298

United States Department of Energy. 2015. Carbon Dioxide Information Analysis Center website. Available from http://cdiac.ornl.gov/trends/co2/graphics/delta_13c_in_co2.html. Accessed September 13, 2015.

Warner, N. R., T. M. Kresse, P. D. Hays, A. Down, J. D. Karr, R. B. Jackson, and A. Vengosh. 2013. Geochemical and isotopic variations in shallow groundwater in areas of the

Fayetteville shale development, north-central Arkansas. Appl. Geochem. **35**: 207–220. doi:10.1016/j.apgeochem.2013.04.013

Waseda, A. 1998. Organic carbon content, bacterial methanogenesis, and accumulation processes of gas hydrates in marine sediments. Geochem. J. **32**: 143–157. doi:10.2343/geochemj.32.143

Whiticar, M. J. 1999. Carbon and hydrogen isotope systematics of bacterial formation and oxidation of methane. Chem. Geol. **161**: 291–314. doi:10.1016/S0009-2541(99)00092-3

Whiticar, M. J., and E. Suess. 1990. Hydrothermal hydrocarbon gases in the sediments of the King George Basin, Bransfield Strait, Antarctica. Appl. Geochem. **5**: 135–147. doi:10.1016/0883-2927(90)90044-6

Xia, X., and Y. Tang. 2012. Isotope fractionation of methane during natural gas flow with coupled diffusion and adsorption/desorption. Geochim. Cosmochim. Acta **77**: 489–503. doi:10.1016/j.gca.2011.10.014

Zhuang, G. C., F. J. Elling, L. M. Nigro, V. Samarkin, S. B. Joye, A. Teske, and K. U. Hinrichs. 2016. Multiple evidence for methylotrophic methanogenesis as the dominant methanogenic pathway in hypersaline sediments from the Orca Basin, Gulf of Mexico. Geochim. Cosmochim. Acta **187**: 1–20. doi:10.1016/j.gca.2016.05.005

Acknowledgments

The authors would like to thank Hamilton College students Rachel Green, Daniel Licthenauer, Matthew Bzurstoski, Kevin Boettenger, Robert Clayton, Helen Farrell, Leonard Kilekwang, Christopher Rider, and Andrew Serachick for their assistance during sample collection and processing, the Hamilton College Dean of Faculty for providing student summer research stipends, the New York State Parks, the Green Lakes State Park staff and Rangers in particular for their help, and the NASA Astrobiology Institute, the Penn State Astrobiology Research Center, the NASA Postdoctoral Program, and NSF Grant EAR-1349258 for their generous support. The authors would also like to thank Aviv Bachan for help in setting up 1D diffusion models for DIC and CH_4 in the FGL water column. T. L. H. graciously acknowledges support from the NAI Postdoctoral Program and the University of Cincinnati. J. R. H. would like to thank Chris House for support, use of laboratory equipment and space, encouragement, and helpful conversations, and the University of Cincinnati for support. The authors also appreciate the thoughtful comments of three anonymous reviewers.

Conflict of Interest

None declared.

Submitted 16 November 2016
Revised 29 April 2017
Accepted 17 June 2017

Associate editor: Caroline Slomp